Quantum transport in chaotic and integrable ballistic cavities with tunable shape

Y. Lee, G. Faini, and D. Mailly
CNRS, Laboratoire de Microstructures et de Microélectronique, 196 Avenue Henri Ravéra, Boîte Postale 107, 92225 Bagneux Cedex, France

(Received 1 July 1996; revised manuscript received 21 January 1997)

We have performed magnetotransport measurements in ballistic cavities and obtained the average by small modulations on the shapes and/or on the Fermi level. We work with cavities whose underlying classical dynamics is chaotic (stadia and Sinaï billiards) and integrable (circles and rectangles). The former show a Lorentzian weak-localization peak, in agreement with semiclassical predictions and other averaging methods that have been used in recent measurements. For integrable cavities our measurements show that the shape of the weak localization is very sensitive to the exact geometry of the sample: a linear magnetoconductance has been observed for rectangles as expected by the theory for integrable cavities, whereas for circles the shape is always Lorentzian. These discrepancies illustrate the nongeneric behavior of scattering through integrable geometries, that we analyze taking into account the interplay of integrability with smooth disorder and geometrical effects. The power spectra of the conductance fluctuations are also analyzed, the deduced typical areas are in good agreement with those obtained from the weak localization. Periodic orbits in nonaveraged Fourier transforms of the magnetoconductance for regular cavities are clearly identified indicating the good quality of our samples. [S0163-1829(97)02439-9]

I. INTRODUCTION

The transport in microstructures has been intensively studied for more than ten years and has shed a new light on our understanding of the notion of conductance. The first studies where mainly devoted to the diffusive regime, where beside the presence of impurities, electrons can preserve phase coherence and experience interferences on a much larger distance than the elastic mean free path. These interference effects lead to the observation of the Aharonov-Bohm oscillations, the universal conductance fluctuations or the persistent current in a solid.[1] Shortly after these first pioneer works, the improvements in the quality of the growth of semiconductors (mainly for the III-V compounds) and in the lithographic methods have allowed physicists to perform experiments on samples with a size smaller than the elastic mean free path. This ballistic transport has shown many new features, like the quantization of the conductance in a quantum point contact (QPC) (Ref. 2) or the electron focusing by a magnetic field.[3] The first indication on the importance of the shape was in the work on the quenching of the Hall effect[4] where the rounding of the corners of the Hall bar was the principal ingredient to explain the focusing of the electrons suppressing the classical Hall effect.

Here, we discuss the ballistic transport in a very different approach. We will consider the exact shape of the sample and analyze the implication of the interferences of the specularly scattered electron waves by the edges of the sample on the transport properties. This question is also motivated by developments in the chaos community where quantum experimental systems are rare.

The idea is to study how the classical dynamics affects the quantum properties or equivalently what is the connection between classical trajectories and quantum mechanics. This is the aim of the quantum chaos. Most of the works in quantum chaos discuss the relation between the classical dynamics and the energy-level statistics since the quantization of the energy level is the most obvious signature of quantum mechanics. Transport in ballistic cavities is a scattering problem and therefore one deals with a continuous spectrum. In this case, scattering properties of the electron through the cavities will be the quantities related to the classical dynamics of the system.

Classically, the essential difference in the dynamics between chaotic and regular structures is the exponential sensitivity to the initial conditions for the former. This signature of chaos is difficult to observe in the transport properties since one cannot inject a sharp enough electron distribution in the cavity. On the other hand, the comparison between chaotic and regular structures can be done through the magnetic-field dependence of the quantum transport. Semiclassical theories have been developed to calculate the magnetoconductance and its quantum corrections. The essential hypothesis for the semiclassical theory in this case is that N, the number of channels entering the cavity, is very large. The starting point of the theory is to calculate the transmission of the mode m entering the cavity and leaving it into the mode n, and then the conductance through the Landauer formula.[1,5,6] Semiclassically, each transmission amplitude is written as the product of an amplitude times a phase. This phase can be expressed as the classical action accumulated by the electron when traveling through the cavity. This way of connecting the classical dynamics to the quantum properties, is analogous to the well-known Gutzwiller trace formula[7] expressing the density of states of a closed system. Within this formulation, the relevant difference between chaotic and regular structures is that concerning the distribution of lengths and enclosed areas of the scattering trajectories. Both distributions follow an exponential law for the chaotic case, while a power law is found for integrable geometries. It is worthwhile to note that only chaotic systems have a generic behavior whereas for regular systems the exact shape

of the particular structure plays an important role, leading to only qualitative predictions. See Ref. 5 and references therein for reviews.

In this paper, we will show experimental results on the transport in chaotic and nonchaotic cavities. We have observed a line-shape typical for nonchaotic dynamics in the case of rectangle structures for the averaged magnetoconductance. All the other studied structures, namely, stadium, circle, and Sinaï billiard show a Lorentzian shape, which is expected for a chaotic system. The unexpected finding of a chaotic signature in the case of the circle is discussed in the light of previous experimental results. The power spectrum of the magnetoconductance is also analyzed and the typical areas extracted show a systematic increase for the regular cavities compared to the chaotic ones. This shows that the two dynamics are different even if the Lorentzian shape for the circle indicates the presence of chaos. Finally, we show that the nonaveraged Fourier spectrum of the circle exhibits high-frequency components which can be linked to periodic orbits since they are annihilated by changes in the cavity shape. This clearly demonstrates the presence of periodic orbits in quantum ballistic cavities.

II. SAMPLES AND EXPERIMENTAL TECHNIQUE

We have fabricated ballistic cavities using the $Al_xGa_{1-x}As$-GaAs system. The distance of the two-dimensional electron gas (2 DEG) from the surface in our modulated-doped heterostructure is 120 nm. When cooled down to liquid-helium temperature the 2 DEG has an electron density $n=2.5\times10^{11}\ \mathrm{cm}^{-2}$ and a mobility $\mu=1.2\times10^{6}\ \mathrm{cm}^{-2}\,\mathrm{V}^{-1}\,\mathrm{s}^{-1}$. These values yield to a Fermi wavelength $\lambda_f=50$ nm and an elastic mean free path $1_e=7\ \mu$m. The shapes of the cavities are defined by shallow ion etching using 200 V argon ions and an aluminum mask patterned by electron-beam lithography. Care has been taken in the design in order to avoid direct paths through the structure. Different geometries have been investigated: circles, rectangles, stadia, and Sinaï billiards. The first two having a regular dynamics while the others are chaotic. A scheme of these structures is drawn in Fig. 1, whereas a scanning electron microscopy (SEM) micrograph of each cavity is shown in the insets of Figs. 3–5, 7, and 12. The effective areas for the circle and the two chaotic structures is 1.3 $\mu\mathrm{m}^2$ while it is 0.9 $\mu\mathrm{m}^2$ for the rectangular one. These values include a lateral edge depletion of 0.1 μm due to the etching process. The lateral depletion is measured using weak-localization corrections on a set of parallel wires of different widths processed on the same samples.[8] From these measurements a coherence length of 20 μm is also extracted. The size of all the samples is much smaller than both the elastic mean free path and the coherence length, yielding to a fully coherent ballistic transport. Then, by lift-off of Ti/Au, we deposit two types of gates on the structure. The first type is used to select the electron channel number entering and leaving the structure. Each of them consists of split gates placed on the leads connecting the cavity to the measuring probes. Such a design allows us to separate the selection of the channel number from the shape of the cavity, which is defined by the etching process. The second type of gate is located directly on the top of the cavity allowing us to change *in situ* the shape or the Fermi level in order to average the conductance. For chaotic cavities, the shape of the central gate is not relevant, whereas for the regular one this central gate must preserve the integrability of the geometry. This is important in order to not switch from a regular to a chaotic behavior when sweeping the gate voltage. The central gate for the circle is then circular (inset of Fig. 4). For the rectangle, the central gate is located on one side (inset of Fig. 5). The gate voltage slightly changes the size of the rectangle, but not its dynamics.

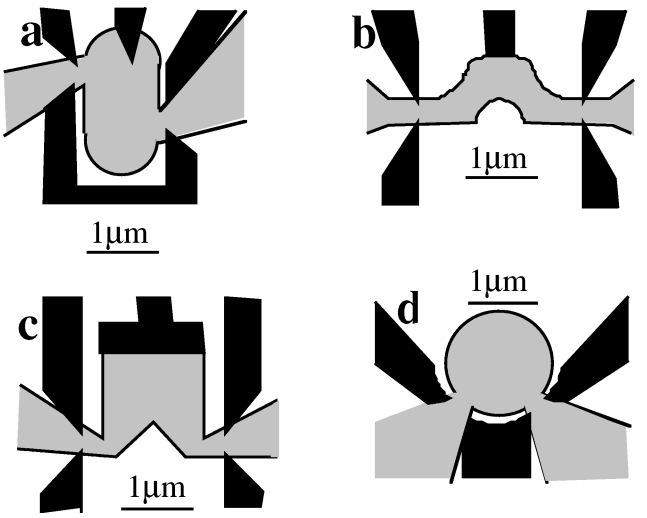

FIG. 1. Schematic drawing of the geometries of the different cavities investigated in this work: (a) stadium, (b) Sinaï billiard, (c) rectangle, and (d) circle (the circular top gate is not shown here for clarity).

An essential condition to be fulfilled in order to compare the different shapes is the good specularity of the bouncing of the electrons on the boundaries of the cavity. Diffusive reflections will always lead to chaotic dynamics whatever the geometry is. To probe the good quality of the boundary reflections we have designed the same chip bend resistance measurement samples.[9] These samples are multiterminal Hall barlike configurations. The current is injected between two orthogonal leads next to each other, whereas the voltage probes are placed outside the current leads at various distances from them. The measurement of the decrease of the voltage versus the distance together with the magnetoresistance allows us to determine the specularity coefficient: we find 85%. This value is similar to those obtained by Roukes *et al.*[9]

Samples are placed on the cold finger of a dilution fridge at $T=0.1$ K. A perpendicular magnetic field can be swept with a minimum step of 0.03 mT. Measurements are recorded using an ac resistance bridge working at 33 Hz with an injection of 1 nA. Most of the results reported in this paper are collected in the low number of electron channel mode, i.e., $N=2$ and 3. The major reason is that the escape time is directly related to the ratio between the perimeter of the cavity and the width of its connections; therefore, in order to have a small cavity with a good ''trapping'' we need small entry widths.

Because of the appearance of the Shubnikov–de Haas oscillations at about a magnetic field of 250 mT we restrict the sweep in magnetic field below this value. A typical magne-

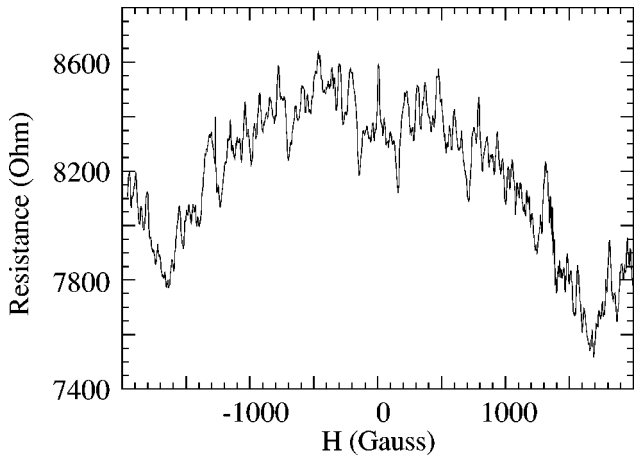

FIG. 2. Typical magnetoresistance trace for a circle at $T = 100$ mK.

toresistance of a circle is plotted on the Fig. 2. In most of the traces, a peak in the magnetoconductance is observed near zero magnetic field although large fluctuations occur when sweeping the magnetic field. In order to extract the exact shape of the backscattering peak we need to average the signal. This is done with the help of the central gate. Several magnetoconductance traces are recorded by changing the central gate voltage enough to decorrelate the conductance fluctuations of two consecutive measurements. This allows us to create many ensemble members, typically 15 traces, and to extract the ensemble-averaged backscattering peak.

III. AVERAGE CONDUCTANCE

Similarly to the case of diffusive systems, semiclassical theories predict for ballistic systems a quantum correction to the classical conductance due to the coherent backscattering of exactly time-reversed paths. The dependence of this correction with the magnetic field can be inferred from the knowledge of the area distribution. In the chaotic case, a Lorentzian shape is predicted:[5]

$$\langle G(B)\rangle = \langle G(0)\rangle - \frac{\Delta G_{BS}}{1+\left(\frac{2B}{\alpha\phi_0}\right)^2}, \qquad (1)$$

where ϕ_0 is the elemental flux quantum and α is the inverse of the area enclosed by a typical trajectory which governs the exponential proliferation of the trajectories with the effective area, $N(\Theta)\propto\exp(-\alpha|\Theta|)$.[6] One should note that α^{-1} can be substantially larger than the size of the cavity since the particles bounces many times on the boundaries before escaping. Thus, more flux than one flux quantum is accumulated along a typical trajectory through the cavity.

Nonchaotic systems do not exhibit an exponential distribution of the effective areas, therefore a different shape for the magnetoconductance is expected. In addition, in integrable systems the distributions may have a significant dependence on the angle of the incident electrons and the conductance dependence must be evaluated by direct simulations on the exact shape. A linear shape of the backscattering peak has been computed for some peculiar regular geometries.[5]

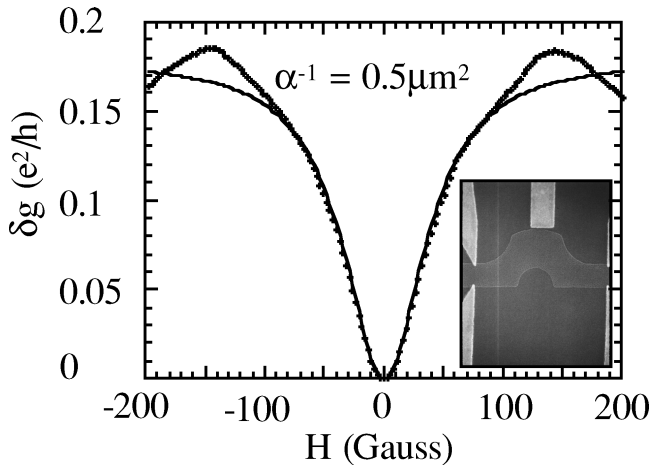

FIG. 3. Averaged magnetoconductance of a Sinaï billiard in units of e^2/h. Pluses are the experimental points, solid line the Lorentzian fit using Eq. (1): the α^{-1} value deduced from the fit is 0.5 μm^2. The inset shows a SEM micrograph of the cavity.

This backscattering peak as been observed in all the experimental works[10–16] in ballistic transport, but Chang *et al.*[11] was the first group, and up to now the only one, to observe a difference in the line shape of the peak between regular and chaotic structures. They measured arrays of stadia and circles in order to average the magnetoconductance and wash out the fluctuations. A Lorentzian-shaped peak was observed for the stadia whereas a more triangular signal was measured for the circles. All the other attempts were not successful, Berry *et al.*[13] with a circular cavity, Keller *et al.*[16] with a polygonal cavity, and Lutjering *et al.*[17] with rectangle cavities, all of them found a Lorentzian line shape.

Figures 3 and 4 show a plot of the averaged magnetoconductance for the Sinaï billiard and the circle. No significant difference in the line shape is observed. For all data obtained with the chaotic samples and the circle, we find a good agreement with the Lorentzian fit (solid lines on the figures). The major difference between these samples lies in the typi-

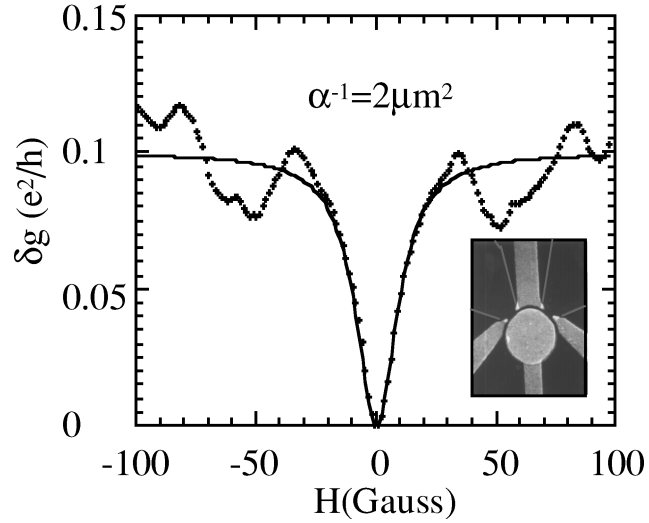

FIG. 4. Averaged magnetoconductance of a circle in units of e^2/h. Pluses are the experimental points, solid line the Lorentzian fit using Eq. (1): the α^{-1} value deduced from the fit is 2 μm^2. The inset shows a SEM micrograph of the cavity.

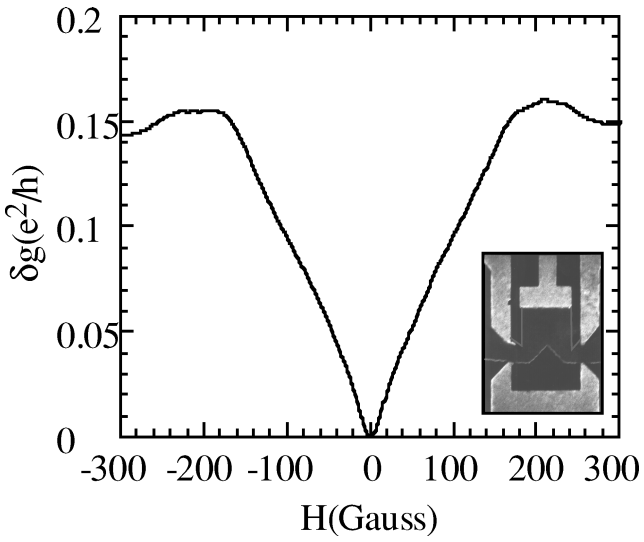

FIG. 5. Averaged magnetoconductance of a rectangle in units of e^2/h, showing a linear behavior. The inset shows a SEM micrograph of the cavity.

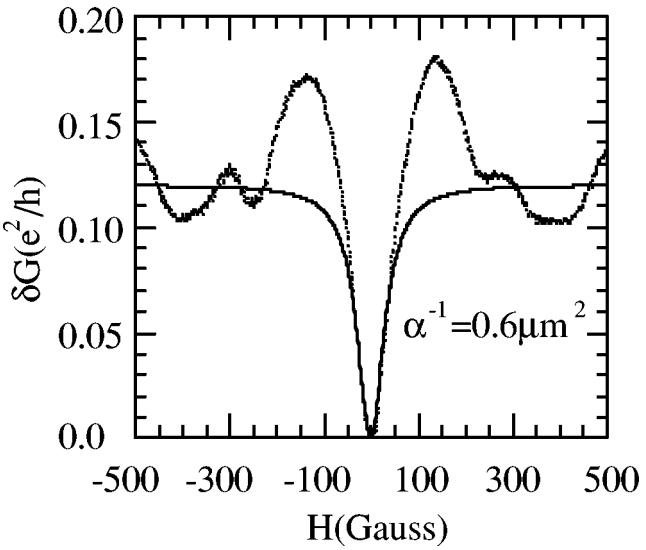

FIG. 6. Same as in Fig. 4 for a smaller circle having a diameter of 0.75 μm. The α^{-1} value deduced in this case is 0.6 μm^2.

cal enclosed areas deduced from the fit with Eq. (1). Although the geometrical areas are identical, we found $\alpha^{-1} = 2$ μm^2 for the circle and 0.5 μm^2 for both the stadium and the Sinaï billiard. This higher value for α^{-1} for the regular dynamic, which is the signature of the presence of large periodic orbits, have been also observed.[13]

In Fig. 5 we show the same plot for a rectangle. A Lorentzian fit does not hold for these data. The weak-localization correction has a clearly linear behavior as expected by theory. This result for the rectangle is very similar to the one Chang *et al.* obtained for the circle.[11] Surprisingly, they also try the rectangular shape and they do not observe the linear magnetoconductance. Our result is then, in one sense, in contradiction with what they obtained but on the other hand, it is a confirmation of the possibility to experimentally probe the dynamics through the backscattering correction. Many reasons can be invoked to understand a Lorentzian behavior observed for an integrable system.

The weak-localization peak depends on the area distribution. The triangular shape of the peak is a signature of a power-law distribution for large θ. Any perturbation that cuts off or alters the large-θ part of the distribution will then break the triangular character of the weak-localization peak. Finite temperature gives rise to a cut off for the length of relevant classical trajectories, through inelastic processes and the rounding of the Fermi surface. A small amount of disorder, an imperfect specularity of the walls, or some geometrical imperfections altering the integrability of the dynamics will drive the area distribution away from a power law. In addition, the injection angle may be relevant for the area distribution in integrable cavities. Varieties of these effects have been invoked to explain the fragility of the integrable behavior.

The assumption of residual impurities was given to explain a Lorentzian line shape also in nonchaotic cavities.[16,17] In order to test this effect in our experiments, we have reduced the size of the circle down to 1.0 μm and 0.75 μm in diameter and we have not obtained any change for the results (except of course a reduction of α^{-1}). Figure 6 shows, for example, the weak-localization correction for the 0.75 μm diameter circle together with the Lorentzian fit giving a $\alpha^{-1} = 0.6$ μm^2. This rules out the effect of a too small mean free path. One can also argue that the time of escape in the cavity which is given by the ratio of the perimeter of the cavity with the size of the opening can be important and leads to trajectories larger than the elastic mean free path or even the phase-coherence length. For the 1.3 μm^2 circle this ratio is such that a typical trajectory needs 13 bounces before escaping for $N=3$ and gives a typical length of about 15 μm. This value is larger than the mean free path and might be an explanation for our result on the circle. But the mean free path is an average quantity and one can ask what is the meaning of an elastic mean free path of 7 μm in a single cavity of about 1 μm diameter. The same analysis for the small circle yields to five bounces for $N=3$ and a typical trapped trajectory of 3 μm much less than 1_e. The fact that the shapes of the weak-localization correction are identical indicates, in our sense, that the mean-free-path argument is not relevant. Furthermore, the typical enclosed areas α^{-1} scale with the geometrical area of the cavities: the ratio of the former is 3.3 and the ratio of the latter 3.9.

Another important point is to ensure that the voltage variations on the gate, which is our way to average the signal, do not produce any important change on the geometry of the circle. We check this point by a local averaging of the magnetoconductance in the two extremities of the gate voltage exploration without finding a significant difference in α^{-1}. Furthermore, the averaged Fourier transforms of the signal at the two extreme gate voltages used are fully superposable (see Sec. IV), therefore, the classical mechanics is not altered by our averaging procedure.

Interferences between short paths can also give rise to particular magnetotransport effects. As one can easily see from the drawing of the cavities (Fig. 1) direct paths in the case of circles are possible, whereas in the case of the rectangle, it was possible in the design to avoid such trajectories with the central triangular notch without affecting the dynamic. In addition, the influence of the connections onto the cavity has been observed by Bird *et al.*[15] These authors have

shown that a change in the lead geometry can switch the backscattering peak from a Lorentzian to a linear dependence.

Finally, a fine analysis of the classical mechanics of the circle shows that the distribution of areas contains an exponential decay at the beginning before being a power law.[18] Therefore the weak localization in the circle depends on the relationship between this switching length and the length cutting off the integrable behavior. A simulation of the transport properties of our cavities including connections will be undertaken in the near future. This will clarify the case of the circle.

IV. CONDUCTANCE FLUCTUATIONS

Fluctuations around the average conductance are characterized by their amplitude and their power spectrum. Semiclassical treatment of the power spectrum leads to a qualitative difference in the shape of the spectrum of chaotic and nonchaotic structures. More precisely, for chaotic systems one finds[5,6]

$$S_B(\nu)=S_B(0)(1+2\pi\alpha\phi_0\nu)e^{-2\pi\alpha\phi_0\nu}, \tag{2}$$

where ν is the magnetic frequency in cycle/Tesla. Equivalently, the correlation function in magnetic field can be written as

$$C_B(\Delta B)=\frac{C_B(0)}{\left[1+\left(\frac{\Delta B}{\alpha\phi_0}\right)^2\right]^2}. \tag{3}$$

The field scale for the correlation function is twice the one for the average conductance [Eq. (1)] because here the relevant phase involves the difference of two areas while the backscattering correction involves the sum. Again, in the case of nonchaotic systems there is no generic analytic derivation for the power spectrum, but a smaller decay, i.e., a power law, is expected.

In the experimental studies one can always fit the power spectrum with an exponential decay (2) independently of the dynamics.[10,12,13,19] The main difference between the two dynamics relies on the departure of data from the fit that appears earlier in the regular case and the slope of the decay that depends on α^{-1}.

To extract the power spectrum we divide each trace into 256 point intervals, Fourier transform, and average. This is done for several central gate voltages. Figures 7 and 8 are the measured power spectra for a stadium and a circle billiard, respectively. The solid lines show the fit with Eq. (2), using the α values obtained from the weak-localization width. The agreement with the experimental data is satisfactory although we can fit only two to three decades as in other works.[10,11,14] This agreement for the values of α deduced from two different mechanisms gives good confidence with the semiclassical theory. As a way to ensure that the classical mechanics of our structures does not change through our average procedure of the previous section, we verified the correspondence between the values of the α obtained on the two extrema of the gate voltage.

We stress here that the semiclassical approximation is not well justified in the few channels mode. This is shown for the circle (Fig. 8), for instance, where for $N\approx 1$ the departure from the exponential decay is more pronounced. This restriction to a small channel number is always present in experimental studies as opposed to analytical expansions since the finite value of the mean free path limits the size of the cavities, and hence restrains the size of the apertures to avoid direct trajectories and small escape times.

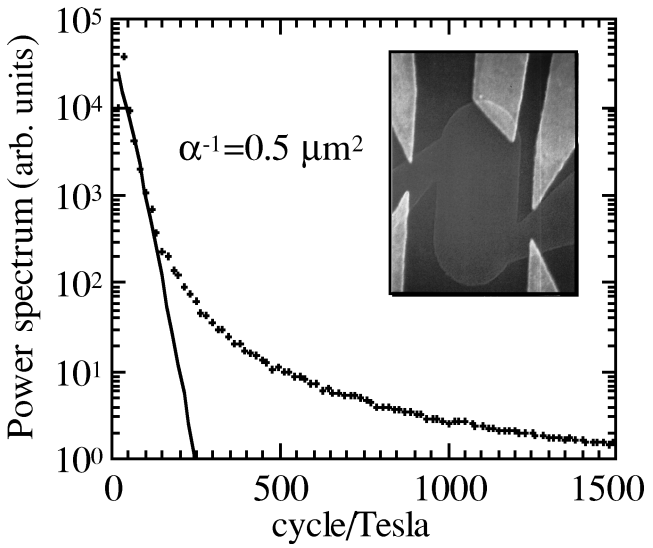

FIG. 7. Power spectrum of the fluctuations for the stadium. Pluses are the experimental points, solid line the fit using Eq. (2) with the α value deduced from the fit of the backscattering dip correction. The inset shows a SEM micrograph of the cavity.

Similar results were obtained for the rectangle and the Sinaï billiard. Figure 9 summarizes the data collected for the power spectrum for the four geometries. For the rectangle we scaled the abscissa in order to take into account the difference in area. Clearly, the two dynamics have a different behavior. The regular samples have, on the one hand, a much richer harmonic spectrum and, on the other hand, a larger value of α^{-1}. This is also consistent with the theoretical

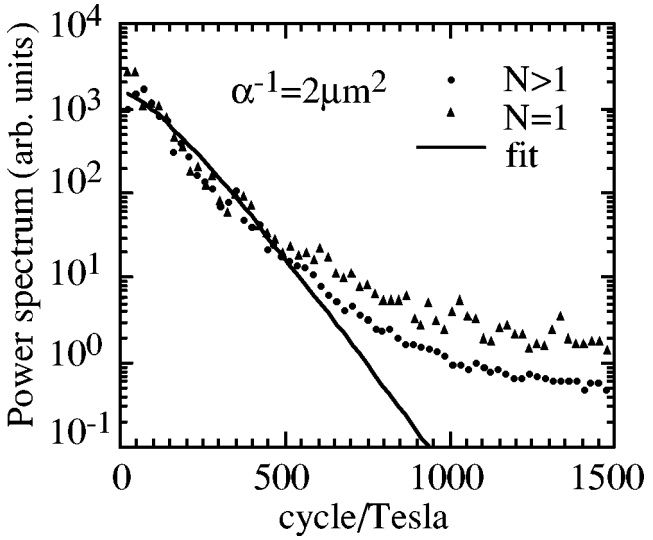

FIG. 8. Power spectrum of the fluctuations for the circle. Closed symbols are the experimental points for a channel number $N\approx 1$ (●) and >1 (▲), solid line the fit using Eq. (2) with the α value deduced from the fit of the backscattering dip correction.

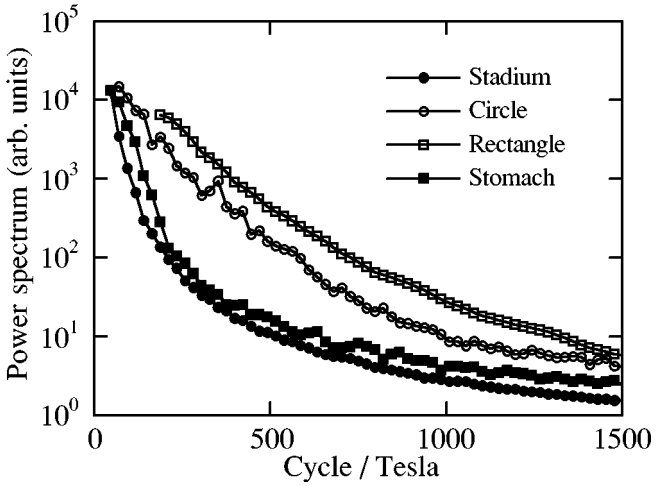

FIG. 9. Power spectra for the four geometries investigated. Abscissa of the data collected for the rectangle have been scaled to take into account the difference in area.

descriptions. A complementary test is given by the correlation function from which we extract, using Eq. (3), typical enclosed area values similar to those obtained by the weak-localization width. This is shown on the Fig. 10 where this correlation is plotted together with the fit for the Sinaï billiard.

V. AMPLITUDES OF THE INTERFERENCE EFFECTS—RANDOM-MATRIX THEORY

All derivations of semiclassical theory only compute one part of the transmission coefficient, namely, the diagonal part in channel number. The conjecture is that all contributions will keep the same shape and this is supported by numerical simulations with chaotic dynamics.[6] It follows that the amplitude of the fluctuations cannot be obtained through semiclassical theory. Random-matrix theory (RMT) has been successfully used to compute the amplitude of the interference effects but only for chaotic systems. The reason for this limitation is that the phase space of the system must be equally filled in order to apply RMT. This happens only in the case of chaotic structures because of the exponential proliferation of the trajectories, whereas in regular systems, strong periodic orbits populate only part of the phase space. The main results of RMT applied to ballistic transport are listed below.[20,21]

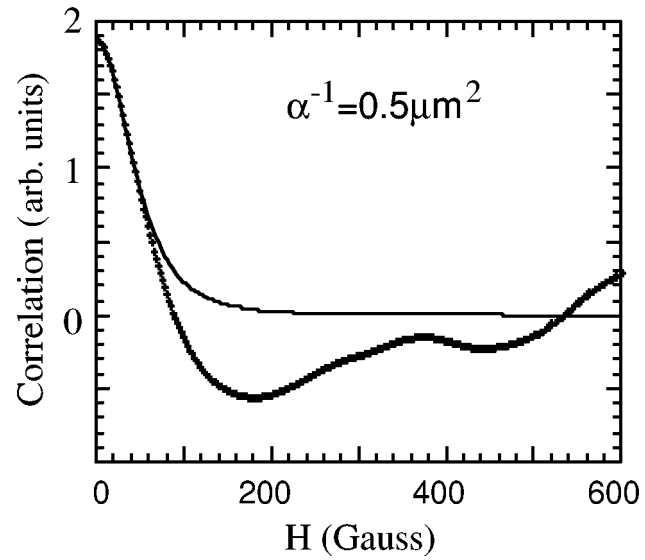

FIG. 10. Correlation function for the Sinaï billiard. Pluses are experimental points, solid line the fit using Eq. (3). The α^{-1} value of 0.5 μm^2 deduced from this fit is the same as that deduced from the backscattering peak (see Fig. 3).

$$\langle g\rangle - \frac{N}{2} = -\frac{N}{4N+2}\,\delta_{1,\beta} \to -\tfrac{1}{4}\delta_{1,\beta} \quad \text{when } N\to\infty, \tag{4}$$

$$\mathrm{var}(g) = \frac{N(N+1)^2}{(2N+1)^2(2N+3)} \to \tfrac{1}{8}$$

$$\text{when } N\to\infty,\ \beta=1,\ \text{COE}, \tag{5}$$

$$\mathrm{var}(g) = \frac{N^2}{4(4N^2-1)} \to \tfrac{1}{16} \quad \text{when } N\to\infty,\ \beta=2,\ \text{CUE}, \tag{6}$$

where g is the conductance in units of e^2/h, δ is the Kronecker symbol, and β determines the symmetries of the ensemble. COE and CUE stand for the circular orthogonal and unitary ensemble, respectively. The universal behavior (similar to that of the diffusive systems) is only recovered for the large number of channels. Nevertheless, these equations are quite disappointing for an experimentalist since the variations of var(g) versus the channel number are small, even in the extreme quantum limit, i.e., $N=1$. Fortunately, RMT can also compute higher moments and a drastic effect appears on the distribution of g for small channel numbers:[20] when $N=3$ the distribution of the transmission is almost Gaussian and for $N=2$ and $N=1$ there are strong deviations from the Gaussian, the distribution being almost flat for $N=1$ in the CUE.

Up to now, no evidence of such conductance distribution has been observed. The amplitude of interference effects can only be compared with theory for chaotic systems. For the weak localization we find a correction of 0.25 for the stadium and 0.17 for the Sinaï billiard whereas RMT predicts 0.2 for $N=2$. The rms amplitude of the fluctuations are 0.085 ($B=0$) and 0.04 ($B\neq 0$) for the stadium, whereas for the Sinaï billiard we find 0.065 ($B=0$) and 0.05 ($B\neq 0$). RMT gives 0.32 ($B=0$) and 0.26 ($B\neq 0$) for two channels. The amplitude measured by Marcus *et al.*[22] was also smaller than RMT predictions and phase-breaking channels were invoked in order to explain this discrepancy. The amplitude of the fluctuations that we measure is not universal but depends on the channel number or equivalently on the mean conductance, at odds with the universality of the theoretical predictions. The conductance fluctuations increase with increasing channels number quite strongly. Figure 11 is a plot of the amplitude of the conductance fluctuations versus the channel number (deduced from the average conductance) for the circle and the stadium. The amplitude increases quite strongly for both geometries and this is in contrast with the very small dependence predicted by the RMT. A similar increase has been also observed.[10] Our data can be explained by taking into account the fact that long trajectories do not

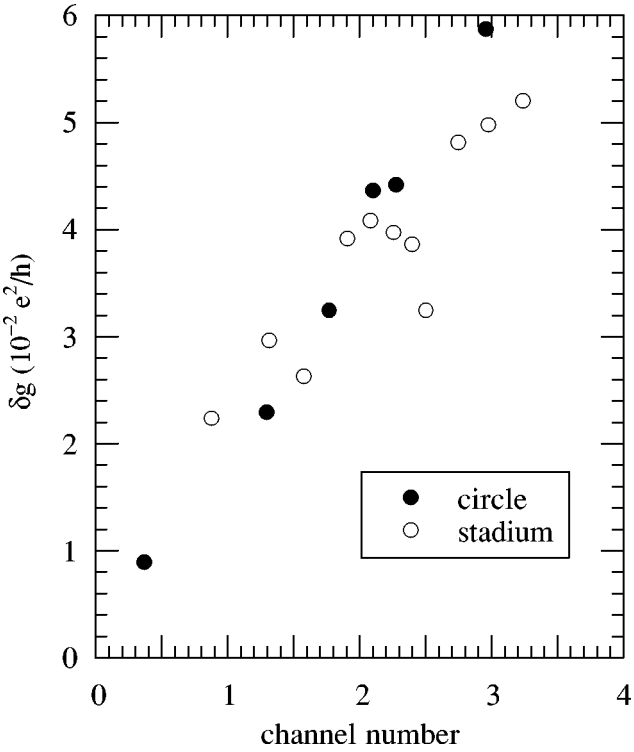

FIG. 11. rms amplitude of the conductance fluctuations vs the channel number for the circle (●) and for the stadium (○). The channel number is deduced from the averaged conductance.

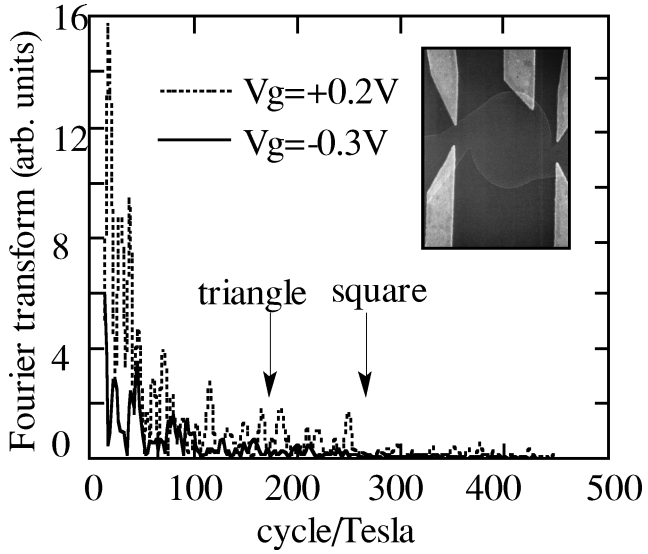

FIG. 12. Nonaveraged Fourier transform of a circle with a central gate designed in such a way to switch from a regular to a chaotic dynamics (SEM micrograph of the circle is shown in the inset). Solid and dotted lines are the spectra for a negative and a positive voltage bias applied, respectively, to the central gate. Arrows indicate the position of the first two strong periodic orbits expected for the circle.

participate in the fluctuations if they are larger than the phase coherence or the thermal length. When the average conductance increases by opening the connections, the escape time decreases leading to a decrease of the weight of the long trajectories on the conductance. This can explain the rise of the fluctuation amplitudes with the channel number. On the other hand, weak localization is already an averaged quantity and is thus less sensitive to phase-breaking effects. RMT describes a linear behavior of the fluctuations with the channel number by introducing phase-breaking channels.[23]

Our investigation of the distribution of the conductance at low channel number needs at the moment more data to be quantitative. First analysis of our preliminary data gives evidence of a strong deviation from the Gaussian distribution as the channel number approaches the unity. The main difficulty is the cross talking of the central gate with the QPC gates, which means that the channel number can slightly vary when one sweeps the central gate voltage and limits the range of available gate voltages, hence limiting our statistics.

VI. DIRECT EVIDENCE FOR STABLE PERIODIC ORBITS

Finally, we can demonstrate that we are able to effectively fabricate nonchaotic systems. We have designed a circle with a central gate in the form of a pie portion (photo in the inset of Fig. 12). In this case, the central gate allows us to switch from a regular to a chaotic dynamics. Figure 12 shows the effect of this gate on the nonaveraged Fourier transform of the magnetoconductance. The dotted line is the recorded signal with a small positive voltage on the gate which ensures that no depletion occurs beneath the gate and the solid one with a negative voltage on the gate which depletes the 2 DEG beneath the gate. We clearly annihilate the high-frequency components corresponding to the shortest periodic orbits when we remove a portion of the pie; low frequencies are only reduced. Arrows indicate the position of the first two strong periodic orbits expected for the circle: the triangle and the square. Peaks appear at a very close position with the full circle and are suppressed when the notch is effective. Rather than claiming that we have identified given sets of periodic orbits, we only stress that the position of the peaks scales with the range of fields expected for periodic orbits in our geometry. For the stadium the central gate has a much weaker effect on the spectrum: mainly the very-low-frequency signals are affected. In Fig. 13 we have plotted the nonaveraged Fourier transform of the stadium and the circle showing the large amount of high frequencies for the circle compared to the stadium (keeping in mind that the areas are the same). One can note that the spectrum of the circle with a negative gate voltage (Fig. 12) is very similar to the one of the stadium (Fig. 13), indicating the change of dynamics with the central gate that eliminates the large area enclosing stable trajectories of the circle.

VII. CONCLUSIONS

We have studied quantum transport in ballistic cavities in the $Al_xGa_{1-x}As$-GaAs 2 DEG. The shape was obtained by ion etching whereas gates deposited on each lead allow us to control the channel number independently from the geometry. The average of the conductance was obtained by small modulations of the shape and/or the Fermi level with the help of an additional gate on the top of the cavity. Different shapes have been investigated: circles, rectangles, stadia, and Sinaï billiards. The backscattering peak shows a linear shape as predicted by the theory for integrable geometries

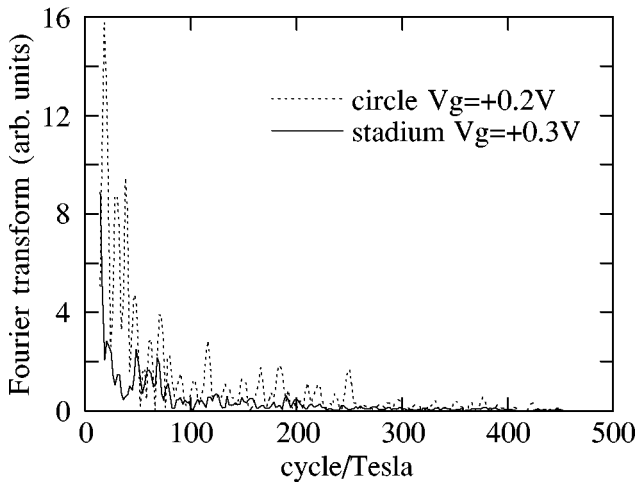

FIG. 13. Nonaveraged Fourier transform of a circle (dotted line, same as in Fig. 13 with a positive voltage bias applied to the central gate) and of a stadium (solid line) with the same area, showing the large amount of high frequency for the integrable cavity.

only for the rectangle structure. Such triangular back scattering peak has been observed up to now only by Chang *et al.*[11] for a circular geometry. A Lorentzian shape is observed for all the other structures. The Lorentzian dependence we have observed for the circle can be attributed to the influence of the contact leads or to the direct paths and to the presence of exponential length distribution for the short trajectories. Numerical simulations on the exact shape of the experimental cavities will be undertaken to settle this problem.

The typical enclosed area deduced from either the weak localization or the power spectrum are the same in all the cases investigated. This typical enclosed area is larger for the regular dynamics than for the chaotic one as expected from their difference in the distribution of areas.

The conductance fluctuations increase sharply by increasing the channel number. This behavior is due to the existence of long trajectories, which vanish when the channel number increases because of the decrease of the escape time.

Finally, we have shown the good quality of our samples by the indication of the presence of short periodic orbits in the circle.

ACKNOWLEDGMENTS

We gratefully acknowledge B. Etienne for molecular-beam epitaxy growth of the samples, C. Mayeux and D. Arquey for technical help. Fruitful discussions with J.-L. Pichard and H. Baranger are kindly acknowledged. We want to thank particularly R. Jalabert for discussions and his comments and criticisms on the manuscript.

[1] For a review see, for instance, S. Whasburn and R. A. Webb, Rep. Prog. Phys. **55**, 1130 (1992).

[2] D. A. Wharam, T. J. Thornton, R. Newbury, M. Pepper, H. Ahmed, J. E. Frost, D. G. Hasko, D. C. Peacock, D. A. Richie, and G. A. C. Jones, J. Phys. C **21**, L209 (1988); B. J. van Wees, H. van Houten, C. W. J. Beenakker, J. G. Williamson, L. P. Kouwenhoven, D. van der Marel, and C. T. Foxon, Phys. Rev. Lett. **60**, 848 (1988).

[3] L. W. Molenkamp, A. A. M. Staring, C. W. J. Beenakker, R. Eppenga, C. E. Timmering, J. G. Williamson, C. J. P. M. Harmans, and C. T. Foxon, Phys. Rev. B **41**, 1274 (1990).

[4] M. L. Roukes, A. Scherer, S. J. Allen, Jr., H. G. Craighead, R. M. Ruthen, E. D. Beebe, and J. P. Harbison, Phys. Rev. Lett. **59**, 3011 (1987).

[5] For a review see H. U. Baranger, R. A. Jalabert, and A. D. Stone, CHAOS **3**, 665 (1993); and H. U. Baranger, *Nanotechnology*, edited by G. Timp (AIP Press, New York, 1996).

[6] R. A. Jalabert, H. U. Baranger, and A. D. Stone, Phys. Rev. Lett. **65**, 2442 (1990).

[7] M. C. Gutzwiller, *Chaos in Classical and Quantum Mechanics* (Springer Verlag, New York, 1991).

[8] D. Mailly, Europhys. Lett. **4**, 1171 (1987).

[9] M. L. Roukes, T. J. Thornton, A. Scherer and B. P. van der Gaag, in *Electronic Properties of Multilayers and Low-Dimensional Semiconductor Structures*, Vol. 231 of *NATO Advanced Study Institute, Series B: Physics* edited by J. M. Chamberlain, L. Eaves, and J. C. Portal (Plenum, New York, 1990).

[10] C. M. Marcus, A. J. Rimberg, R. M. Westervelt, P. F. Hopkins, and A. C. Gossard, Phys. Rev. Lett. **69**, 506 (1992).

[11] A. M. Chang, H. U. Baranger, L. N. Pfeiffer, and K. W. West, Phys. Rev. Lett. **73**, 2111 (1994).

[12] M. J. Berry, J. H. Baskey, R. M. Westervest, and A. C. Gossard, Phys. Rev. B **50**, 8857 (1994).

[13] M. J. Berry, J. A. Katine, R. M. Westervelt, and A. C. Gossard, Phys. Rev. B **50**, 17 721 (1994).

[14] M. W. Keller, O. Millo, A. Mittal, D. E. Prober, and R. N. Sacks, Surf. Sci. **305**, 501 (1994).

[15] J. P. Bird, D. M. Olatona, R. Newbury, R. P. Taylor, K. Ishibashi, M. Stopa, Y. Aoyagi, T. Sugano, and Y. Ochiai, Phys. Rev. B **52**, R14 336 (1995).

[16] M. W. Keller, A. Mittal, J. W. Sleight, R. G. Wheeler, D. E. Prober, R. N. Sacks, and H. Shtrikmann, Phys. Rev. B **53**, R1693 (1996).

[17] G. Lütjerinj, K. Richter, D. Weiss, J. Mao, R. H. Blick, K. von Klitzing, and C. T. Foxon, Surf. Sci. **361**, 709 (1996).

[18] T. Fischaleck, Diploma thesis, University of Augsburg, 1996.

[19] I. H. Chan, R. M. Clarke, C. M. Marcus, K. Campman, and A. C. Gossard, Phys. Rev. Lett. **74**, 3876 (1995).

[20] H. U. Baranger and P. A. Mello, Phys. Rev. Lett. **73**, 142 (1994).

[21] R. A. Jalabert, J. L. Pichard, and C. W. J. Beenakker, Europhys. Lett. **27**, 255 (1994).

[22] C. M. Marcus, R. M. Westervelt, P. F. Hopkins, and A. C. Gossard, Phys. Rev. B **48**, 2460 (1993).

[23] H. U. Baranger and P. A. Mello, Phys. Rev. B **51**, 4703 (1995).